

# Epidermal laser stimulation of action potentials in the frog sciatic nerve

**Nichole M. Jindra**

Air Force Research Laboratory  
2624 Louis Bauer Drive  
Brooks City-Base, Texas 78235

**Douglas Goddard**

**Michelle Imholte**

Northrop Grumman  
4241 Woodcock Drive, Suite B-100  
San Antonio, Texas 78228-1330

**Robert J. Thomas**

Air Force Research Laboratory  
2624 Louis Bauer Drive  
Brooks City-Base, Texas 78235

**Abstract.** Measurements of laser-stimulated action potentials in the sciatic nerve of leopard frogs (*Rana pipiens*) are made using two infrared lasers. The dorsal sides of the frog's hind limbs are exposed to short-pulsed 1540- and 1064-nm wavelengths at three separate spot sizes: 2, 3, and 4 mm. Energy density thresholds are determined for eliciting an action potential at each experimental condition. Results from these exposures show similar evoked potential thresholds for both wavelengths. The 2-mm-diam spot sizes yield action potentials at radiant exposure levels almost double that seen with larger beam sizes. © 2010 Society of Photo-Optical Instrumentation Engineers. [DOI: 10.1117/1.3292014]

**Keywords:** neural stimulation; sciatic nerve; neodymium yttrium aluminum garnet; erbium:glass; infrared; action potential.

Paper 08102RRRR received Apr. 2, 2008; revised manuscript received Sep. 15, 2009; accepted for publication Nov. 24, 2009; published online Feb. 4, 2010.

## 1 Background

Electrical stimulation is commonly used to stimulate action potentials in neurons for both medical and research applications. Electrical signals are applied to a nerve, initiating the voltage change that will start a chain reaction along the axon. Once begun, the signal is passed along the axonal tract. Unfortunately, electrical stimulation systems possess characteristics that create several problems. Besides low spatial specificity (electrical stimulation will activate several nerve tracts simultaneously), difficulties can include tissue damage from electrode installation.<sup>1</sup> Recent studies have found that a laser source can be used to induce an action potential in the nervous system as well as, if not better than, electrical methods. Wells and Kao have shown that there are few differences between optical and electrical stimulation on the activation of the nerves.<sup>1</sup> Laser excitation of neural tissue provides a contact-free, spatially selective, artifact-free method of stimulation without incurring tissue damage.<sup>1</sup> The small spot sizes used by laser systems allow for pin-point accuracy when stimulating nerve tracts, and the low irradiance levels help to minimize introduction of extra energy into the action potential response. Most of the studies were performed directly on the nerves and were within laser-tissue interaction parameters that led Wells and Kao to suspect thermal confinement mechanisms for action potential elicitation.

Clinically, indirect stimulation of nerves has been conducted by radiating the skin with lasers (typically a CO<sub>2</sub> or visible wavelength laser) and activating skin nerve fibers. This technique is typically used for determining pain thresholds, pain desensitization studies, and physiological studies of nociceptive pathways.<sup>2-5</sup> To date, we have been unable to find any data on laser-evoked potentials using nanosecond-pulsed lasers.

This work is a pilot study to determine if action potentials can be induced using near-infrared, short pulses directed through the skin of an animal. Much work has been performed by this laboratory into skin damage thresholds of nanosecond pulsed lasers, and the neural studies mentioned before have led to a desire to clarify whether or not these lasers are causing any unseen neural reactions at low energy levels. Unlike longer pulsed lasers that operate in thermal confinement parameters, ultrashort pulses operate within stress confinement parameters. Thus, any reaction could be thermal, mechanical, or a combination of these or other mechanisms. If they can indeed elicit action potentials, further work will be required to determine the exact mechanism.

Mechanical and thermal receptors are located in the dermis of the skin, and nociceptors are located in both the dermis and deep epidermal layer (see Fig. 1). While most heat receptors activate at ranges just outside of the body's normal temperature, the threshold for onset of a painful sensation is approximately 45 °C—the temperature at which heat produces tissue damage.<sup>6</sup> Signals from each of these receptors travel along peripheral nerves until they reach the central nervous system. Activation of distal receptors can be monitored by measuring impulses at various points along this neural system. In this experiment, skin receptors of the calf were stimulated and neural response was monitored by electrodes imbedded in the peripheral (sciatic) nerve.

### 1.1 Objectives

The goal of this work was to determine the feasibility of an electropotential response of neural receptors due to ultrashort pulsed laser exposures. [All experiments were conducted at Air Force Research Laboratories Human Effectiveness Directorate Optical (RHDO) radiation branch following approval by the Institutional Animal Care and Use Committee (protocol HEDO-06-12).] This was tested during an experiment per-

Address all correspondence to: Nichole M. Jindra, Air Force Research Laboratory, 2624 Louis Bauer Drive, Brooks City-Base, Texas 78235. Tel: 210-536-4850; Fax: 210-536-3903; E-mail: nikki.jindra@yahoo.com

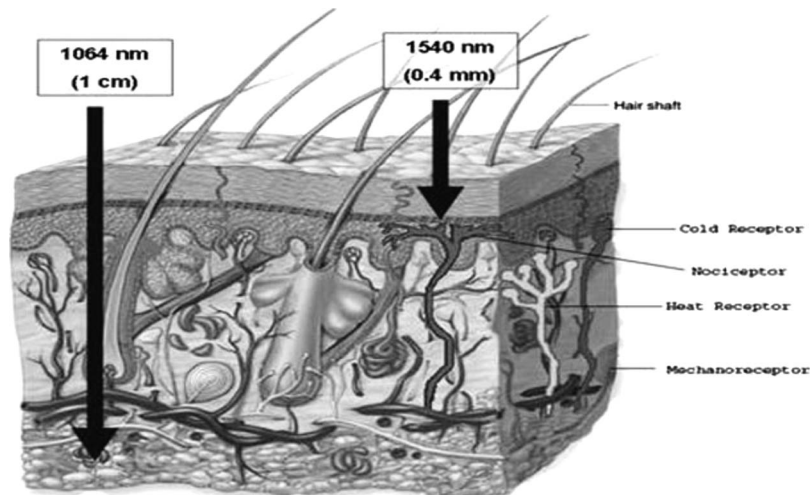


**Fig. 1** Illustration of laser energy penetration and nerve receptor locations in human skin layers. Measurements taken of frog skin for this experiment had a total skin thickness of 0.367 mm.

formed on leopard frogs. An electrode was placed in the sciatic nerve of the frogs to record action potentials elicited from laser exposures on the surface skin of the calf. Three spot sizes and two different infrared wavelengths were used in the study. The data were then analyzed to determine threshold values for action potential stimulations.

## 2 Methods

### 2.1 Leopard Frogs

*In vivo* sciatic nerve experiments were performed using 33 leopard frogs (*Rana pipiens*) from the Carolina Biological Supply Company in North Carolina. The frogs ranged in torso length from 3 to 4 in. and were euthanized via a double pithing technique. To maintain a constant body temperature during the experiment, the cold-blooded frogs were placed on a saline bag that had been warmed to approximately 20 to 22 °C. This was to ensure that the nerve receptors remained within their effective ranges, and that the frogs were not negatively affected by cold ambient temperatures in the laboratory.

Since the subject was an amphibian, the water content of the skin was very high. To minimize variability in the data obtained during this experiment, saline was periodically applied to the skin to maintain hydration. Excess solution was blotted off using gauze.

### 2.2 Nerve Preparation

Nerve preparation started by making a centrally located incision from the knee to the upper thigh, removing the skin from the dorsal side and exposing the trunk of the nerve at the knee. Muscular fascia was incised and removed to expose the rest of the nerve. A piece of latex was placed between the nerve and the underlying muscle to minimize any collateral electrical signals. After the nerve was prepared, insulated stainless steel needle electrodes (Chalgreen Enterprises, Incorporated, Gilroy, California, 111-637-24TP, disposable monopolar EMG needle electrodes, 37 mm × 26 gauge) were inserted into the nerve located approximately 15 mm above the knee. Baseline data were collected to verify the system's iso-

lation from other electrical sources and to ensure correct electrode placement. To initialize each experiment, the sciatic nerve was directly stimulated by the laser to verify that the electrode was reading correctly, and that the nerve had not been damaged by the insertion. Compound nerve action potential (CNAP) responses were recorded with BioPac Systems Incorporated (Goleta, California) MP100 interfaced to a computer running Acknowledge software v3.73. The CNAP is the algebraic sum of many individual "all-or-none" action potentials, arising more or less simultaneously in a large number of individual axons.<sup>7</sup> All action potentials are measured using a differential medical amplifier and extracellular recording electrodes, which measure the summed electrical response of all excited axons in the nerve. The recordings for this project were manually triggered prior to the exposure and recorded 5 sec of data. All signals were amplified 1000 times and electrically filtered with a 50 to 5000-Hz bandpass filter.

Once the initial direct testing of the sciatic nerve had been conducted, the laser was focused on the animal's calf. The surface of the skin was randomly irradiated using varying energy levels, with one minute in-between each shot. This lag time was necessary to prevent overheating of the Er:glass laser and was maintained for both lasers to eliminate unnecessary variation between the exposure procedures.

### 2.3 Laser Setup

Optical stimulation was performed using two infrared laser sources. A Q-switched Nd:YAG laser emitting 1064 nm was first used to verify experimental methods. The Nd:YAG laser was pulsed at a repetition rate of 10 Hz with a pulse duration of 15 ns. Each exposure consisted of just one pulse. The energy of the laser was controlled using a half-wave plate and a polarizing beamsplitter, and the generated pulses were sampled using a 90/10 nonpolarizing beamsplitter by an Ophir LaserStar energy meter using the 1Z0230 power head (Ophir-Spiricon, Logan, Utah). The laser was then directed into a Faraday cage where it would be focused into the desired spot size using a 500-mm biconvex lens. (Fig. 2)

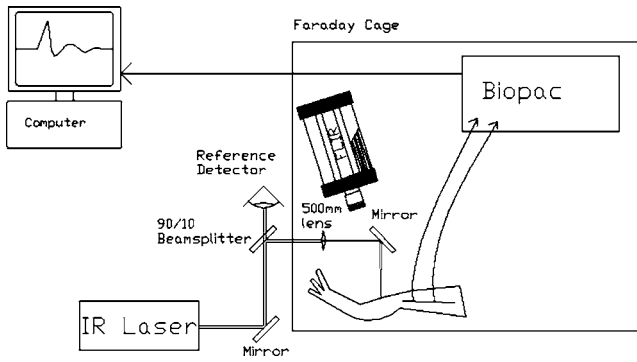


Fig. 2 Generic schematic of experimental setup.

Each infrared laser used possessed a Gaussian spatial beam profile. Beam diameters and profiles were measured using linagraph laser burn paper. Using only one pulse per exposure, three beam diameters were used during the experiment: 2, 3, and 4 mm.

Once the methods were verified with the Nd:YAG laser, an Er:glass (erbium-glass) laser emitting 1540 nm was employed to further evaluate optical stimulation and for statistical comparison with another wavelength. The Er:glass laser was mechanically Q-switched to a pulse duration of 55 ns. Due to the system's high energy, only one shot per minute is allowed. The energy of the laser is varied by adjusting the flash lamp energy. Again, the beam was directed into the Faraday cage and focused to the same spot sizes as with the 1064-nm Nd:YAG laser: 2, 3, and 4 mm.

### 2.4 Probit Analysis

Probit analysis was developed to analyze discrete data collected by experiments involving threshold response rate in biological systems. This is computed using the EZ-Probit program designed by Cain and Manning at Brooks City-Base in San Antonio, Texas.<sup>8</sup> This method has been employed as a statistical tool to determine the probability of dose-response curves for action potential (AP) responses in the sciatic nerve. In this case, the threshold probabilities are reported as AP<sub>50</sub>—the radiant exposure dose that has a 50% probability of creating a response. The values presented here are for 100% probability, without consideration of additional experimental uncertainties. Also, the slope of the probit line is calculated between the ED<sub>84</sub> and ED<sub>50</sub> values. A high value for slope would represent high value for data certainty, with minimal sample-to-sample variability affecting results.

## 3 Results

Data showed considerable variability between the animals in respect to pigmentation placement. While melanin has only a small role in energy absorption at infrared wavelengths, early skin exposures showed noticeable differences between skin damage threshold energy levels for dark and light skin patches. Thus, for greater consistency, only lightly pigmented skin data were used in the analysis. Each AP<sub>50</sub> is represented in units of fluence (J/cm<sup>2</sup>).

A drawback of stimulating nerve receptors through the skin instead of directly on the nerve is that receptors are not

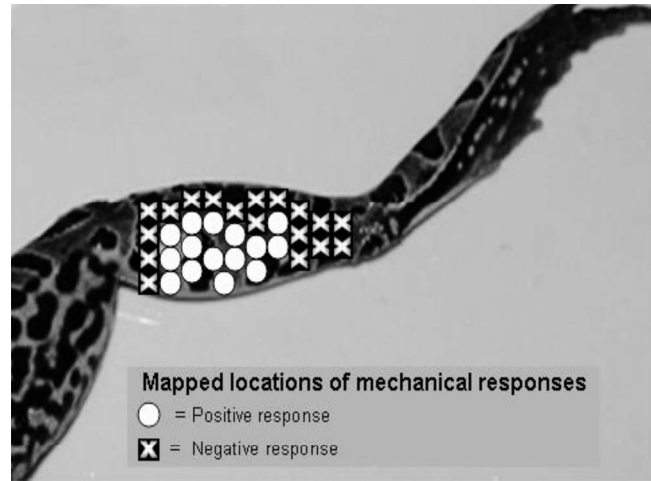


Fig. 3 Mapped locations of frog response areas.

uniformly located across an area. For example, in humans it is known that some areas such as the palms of the hands have very few nerve receptors, whereas other areas, like the tongue or face, have a large concentration of receptors. To get an idea of the distribution on the frog's leg, several frogs were subjected to a consistent irradiance level for multiple exposures across the area. The energy used was high enough to elicit a visual muscular reflex, so that it was not necessary to use the nerve probes. While each frog varied slightly in the actual responses, Fig. 3 shows the general nerve distribution found from this study. The circles were areas where consistent reflex responses were located, while the X's show locations that did not give any reflexive actions. Unfortunately, the scope of this project did not allow for animal dissection or histology to compare anatomical data to the visual cues that were recorded in this study. An examination of this type would be very beneficial for any future studies conducted with this animal model.

Positive responses, such as that seen in Fig. 4, were recorded for every parameter tested in this project. These viable action potentials obtained from the laser exposures are pre-

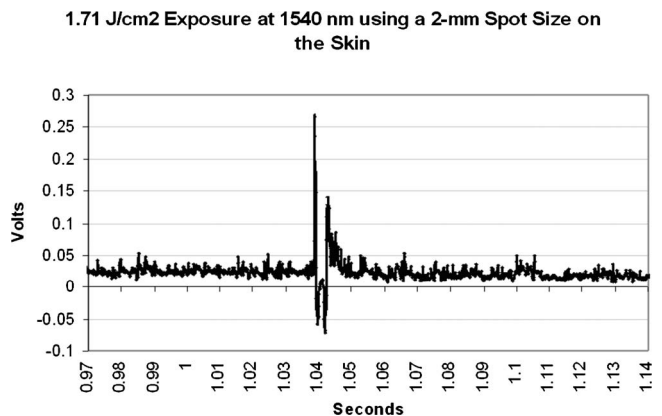


Fig. 4 Action potential elicited from a 2-mm exposure on the frog's calf, using the 1540-nm laser at 1.71 J/cm<sup>2</sup>. Note the secondary action potential that begins 0.03 sec after the laser pulse was initiated. This is likely a motor response that occurs as a result of the exposure.

**Table 1** Action potential thresholds ( $J/cm^2$ ). AP<sub>50</sub> is the energy level at which 50% of exposures will elicit an action potential. UFL=upper fiducial limit. LFL=lower fiducial limit

Spot size	Action Potential Thresholds							
	1064 nm				1540 nm			
	AP50	UFL	LFL	Slope	AP50	UFL	LFL	Slope
2 mm	0.900	1.262	1.470	5.483	1.331	1.838	1.981	74.783
3 mm	0.497	0.557	0.443	25.910	0.449	0.712	0.195	3.423
4 mm	0.430	0.520	0.297	3.678	0.323	0.350	0.296	37.950

sented in Table 1. Measurements were taken from multiple subjects and calculated by combining all data for each spot size and wavelength.

The action potentials elicited demonstrated very similar activation trends among the 1064- and 1540-nm lasers. At each wavelength, the 2-mm spot sizes required approximately  $1 J/cm^2$  of radiant energy to achieve an action potential, versus the larger spot sizes that required less than  $0.5 J/cm^2$  (Figs. 5 and 6). This data also show that the skin became damaged at levels below AP thresholds for both wavelengths when using a 4-mm spot size. The most notable difference between the two lasers was that skin damage occurred below the action potential threshold when using the 3-mm beam at 1064 nm, but not at 1540 nm (Figs. 5 and 6).

#### 4 Discussion

A major impediment to this project was the skin’s tendency to ablate, even at very low energy levels ( $0.169 J/cm^2$ ). As seen in Fig. 7(a), the ablation was inconsistent and varied depending on pigmentation and location of the exposure site. Dark pigmented tissue required less energy and had larger ablation diameters. Thermal data of these areas taken using the forward-looking infrared (FLIR) camera show temperature rises as low as  $0.689 ^\circ C$ , so ablation due to thermal effects is most likely not the reason for this. Many of these low powered exposures did not exhibit the same charred responses around the crater perimeter as the ablations seen with high radiant exposures. [Fig. 7(b)]. The most probably cause, al-

though confirmation of this will require additional experimentation, would be photomechanical damage due to stress confinement.

Thermoelastic expansion of tissue by pulsed laser will eject ablated material through stress wave recoil. Stress waves are produced when optical energy is absorbed into an appropriate medium. If the irradiance is high enough, dielectric breakdown can occur, which leads to the formation of high-pressure plasma and the production of large-amplitude stress waves in the tissue.<sup>9</sup> Shock wave damage effects are due to both compressive and tensile strain. The estimated stress confinement time for this experimental arrangement is 7 and 3  $\mu s$  for 1064 and 1540 nm, respectively, calculated using Eq. (1).<sup>9</sup>

The penetration depth of a Q-switched Nd:YAG laser at 1064 nm is about 1 cm, while the penetration depth of a Q-switched Er:glass laser at 1540 nm is around 1 mm.<sup>10</sup>

One point to remember is that these animals had very high water content in their skin. Not only did this affect energy absorption, it also influenced the amount of heat generated at the exposure site. While we tried to maintain a constant hydration level for the skin, it is possible that some exposures were conducted under drier/wetter conditions than others. To minimize the effects of this, we performed nearly 400 exposures at each spot size. The low temperature changes ( $< 10 ^\circ C$ ) seen at two of the spot sizes used in this study lend credence to our supposition that ablation in those areas was due to stress confinement parameters rather than thermal confinement (Table 2).

As previously stated, the neural response was reliant on the location of the exposures site, probably because of the distri-

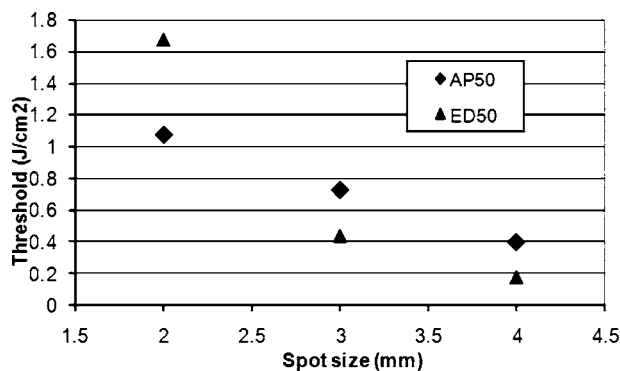


**Fig. 5** Radiant exposure ( $J/cm^2$ ) values for skin damage and action potential thresholds at 1064 nm.

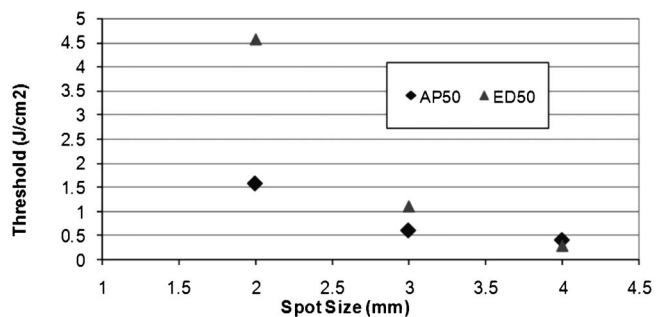


**Fig. 6** Skin damage and action potential thresholds for radiant energy exposures at 1540 nm.

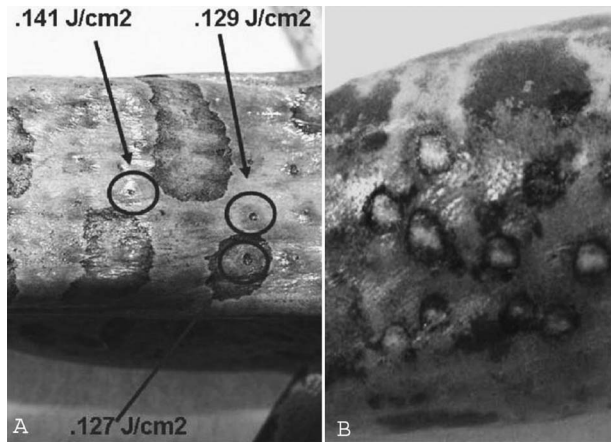


**Fig. 7** (a) Ablation of tissue on the back of the frog. Similar radiant energy levels (0.127 and 0.129 J/cm<sup>2</sup>) show larger amounts of damage for the more heavily pigmented areas than the lightly pigmented areas. (b) Ablation of skin on the dorsal surface of a frog leg. Note the black rings surrounding each crater, potentially indicating charring of the perimeter tissue from thermal effects. Radiant exposure energies varied from 0.386 to 1.12 J/cm<sup>2</sup>.

bution of nerve receptor endings. For exposures using a large spot size, areas with a higher incidence of neural response (as demonstrated by the visual reflex experiments performed in Fig. 3) showed responses at lower irradiance levels than exposures at sites that had lower incidences of response. This could be due, in some part, to activation of more nerve receptors with the larger beam. Additionally, smaller-spot-sized exposures in the same areas showed higher radiant energy levels required to get a neural response. We were unable to find a reference for the distribution of receptors in frog skin.

This project was not able to test the actual area stimulated, only the diameter of the laser beam. If the propagation waves were stress induced, it is possible that the wave continued for some unknown distance outside of that diameter to stimulate receptors nearby.

**Table 2** Spot size versus the average temperature change for each AP<sub>50</sub> value.

1064 nm	
Spot size (mm)	Average delta T (°C)
2	15–20
3	2–4
4	10–15
1540 nm	
Spot size (mm)	Average delta T (°C)
2	6–8
3	20–40
4	40–60

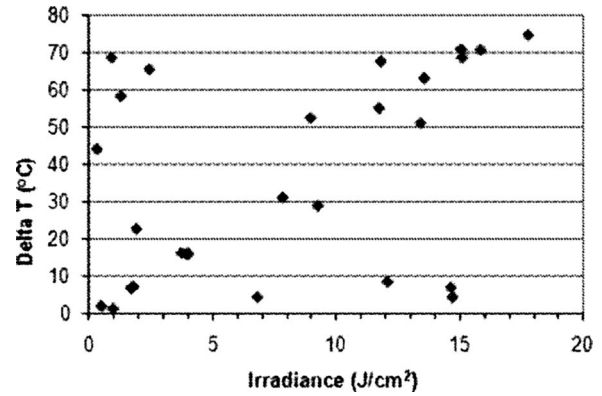


**Fig. 8** Temperature increase data from 2-mm exposures at 1540 nm.

In many of the frogs there were secondary action potentials seen after laser exposure (Fig. 4). The potentials lasted 40 to 70 msec and began 20 to 30 msec after initial exposure. Since these APs coincided with muscle twitches or leg movement of some kind, it is likely that these action potentials are from a motor response. However, the cause of the motor response is unknown. The action could be due to incomplete pithing of those animals, leaving a somatic reflex arc in place. It is also possible that the laser exposure itself somehow elicited an efferent response, as demonstrated in unpublished studies by the University of Vanderbilt.<sup>11</sup> Researchers there have been able to isolate an efferent portion of frog sciatic nerve and stimulate it to make the individual toes move.

Most likely the secondary response was brought on by a delayed response of another kind. Given that mechano- and heat-sensitive A fibers (AMH) and C fibers (CMH) can have response latency periods ranging from 100 ms to several seconds,<sup>12</sup> a potential candidate is that a pain response was brought on by some other factor: thermal, mechanical, or both. As mentioned earlier, this experiment was carried out with parameters within the stress confinement region. AMH and CMH fibers have mechanical thresholds averaging 3.2 bars<sup>12</sup> (46.4 pounds per square inch). With the ablative results of some of the exposures, it is possible that nociceptors were activated by pressure from stress confinement.

Another plausible reason may be a thermal pain response. The action potential seen in Fig. 4 was elicited by a radiant energy level of 1.71 J/cm<sup>2</sup>. Thermal data from these exposures (Fig. 8) show that temperature increases for irradiances of this magnitude were between 5 and 10 °C. Since the frogs were maintained at a temperature of approximately 20 to 22 °C, this would bring the skin temperature to around 32 °C. While this is below the mammalian thermal pain threshold of 44 °C, the temperature increase may have been enough to elicit a pain response. Unfortunately, we did not perform an investigation of the spinal cord severance, nor were we able to perform tests to isolate thermal and mechanical stimuli, so determining the exact mechanism of the secondary response is not possible at this time.

The action potential thresholds achieved at both wavelengths were not very different, despite the distinct penetration depth. This could be due to the thinness of the frog skin; both wavelengths penetrated all the way through the exposed

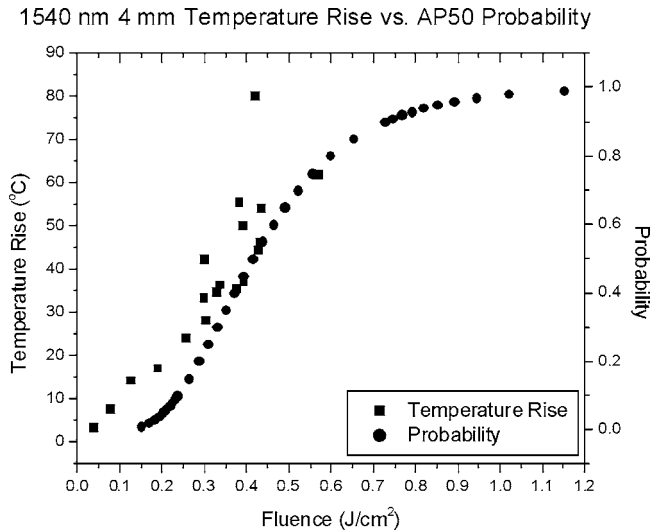


**Fig. 9** AP<sub>50</sub> probability versus temperature rise data for 1540-nm exposures with a 4-mm spot size.

area in many locations. It should be noted again that the thickness of frog skin is much less than that of humans. The average combined thickness of the epidermis, dermis, and subcutaneous layers measured in these experiments was 0.367 mm. This value is approximately the thickness of the human epidermis layer alone.<sup>10</sup> Therefore, it is difficult to draw direct correlation between results achieved in this study to any expected values for human response. For example, an exposure to human skin using the Er:glass laser (penetration depth of approximately 1 mm) would just pass the epidermis, but in the case of the frog it penetrated through all layers of the skin. Murine studies already underway should be able to provide a better representation of human skin, allowing for much clearer results.

While the parameters of this experiment did not provide any conclusive information, the data from the 4- to 1540-nm exposures did provide some insight as to future possibilities for this kind of work. This larger spot size provides for a more linear temperature rise, allowing for more predictable energy requirements to estimate surface damage before exposures (Fig. 9).

## 5 Conclusions

The results presented here are only the beginning of a new line of research in the systematic characterization of neural stimulation with lasers. Once the mechanisms of this laser stimulation are better understood, researchers can begin to develop applications utilizing this technology, such as man-machine interfaces or less-than-lethal weapons.

For this research, we studied the effects at two wavelengths and three individual beam diameters. The most significant finding provided by this study is that smaller beam diameters are needed to avoid tissue damage while still causing stimulation. As the results show, larger beam diameters have much lower thresholds in terms of radiant exposure for both neural stimulation and skin damage. As the laser beam

diameters increase, the damage threshold decreases. The action potential threshold for the larger spots is lower, since the laser is stimulating a greater number of neurons. Therefore, based on our findings, the ideal spot size would be 3 mm, since it requires lower laser energy to stimulate action potentials, and does so at energy levels below those that cause skin damage. It is shown that tissue ablation occurs well before the average surface temperature of the skin reaches 100 °C, which might be explained by laser-induced breakdown or stress confinement mechanisms. Indeed, skin damage frequently occurs before action potentials are stimulated at beam diameters of 4 mm for each wavelength. This phenomenon will certainly require additional studies to determine the exact mechanism of damage, whether it be thermal, mechanical, or a combination of the two.

It became obvious that the differences between frog skin pigmentation and morphology from that of humans makes them ill suited as human skin damage threshold models. A mammalian study (currently underway) should provide the necessary data to determine the best wavelength for creating action potentials without causing skin damage.

Finally, this study is conducted with two wavelengths common in the medical and photonics industries. Additional wavelengths should be studied to determine if different penetration depths or powers could yield more optimal results.

## Acknowledgment

The authors would like to thank Manuel Figueroa for his valuable assistance. His work was crucial to getting this project started. We would also like to thank the Air Force Research Laboratory, Northrop Grumman Information Technologies (contract number F41624-02-D-7003) and Pittsburg State University for their support.

## References

1. J. Wells, C. Kao, P. Konrad, A. Mahdevan-Jensen, and E. D. Jansen, "Biophysical mechanisms responsible for pulsed low-level laser excitation of neural tissue," *Proc. SPIE* **6084**, 60840X (2006).
2. C. Perchet, F. Godinho, S. Mazza et al., "Evoked potentials to nociceptive stimuli delivered by CO<sub>2</sub> or ND:YAP lasers," *Clin. Neurophysiol.* **119**, 2615–2622 (2008).
3. W. J. Kneebone, "Basic principles of low-level laser therapy and clinical applications for pain relief," *Dynamic Chiropractic* **25**(18), 1–7 (2007).
4. K. Moore, "Lasers and pain treatment," *Clinixperience* **2004**, 72 (Feb. 26, 2004), <http://www.lasertpartner.org/lasp/web/en/2004/0072.htm>.
5. L. Arendt-Nielsen and P. Bjerring, "Sensory and pain threshold characteristics to laser stimuli," *J. Neurol., Neurosurg. Psychiatry* **51**, 35–42 (1988).
6. S. Hendry and S. Hsiao, *Fundamental Neuroscience*, 2nd ed., Academic Press, Boston (2003).
7. E. N. Marieb and K. Hoehn, *Human Anatomy and Physiology*, Pearson Benjamin Cummings, New York (2007).
8. C. Cain and L. Manning, "Analyzing yes/no data on a log scale," Tech Report AL/OE-TR-1996-0102, Books City-Base, TX (1996).
9. A. J. Welch and M. J. van Gemert, *Optical-Thermal Response of Laser-Irradiated Tissue*, Plenum Press, New York (1995).
10. S. Jiang et al., "Effects of thermal properties and geometric dimensions on skin burn injuries," *Burns* **28**, 713–717 (2002).
11. J. Wells and D. E. Jansen, Personal Communication (2009).
12. R. D. Treede, R. A. Meyer et al., "Evidence for two different heat transduction mechanisms in nociceptive primary afferents innervating monkey skin," *J. Physiol. (London)* **483**, 747–758 (1995).